SCIENTIFIC REPORTS

OPEN

Permethyl Cobaltocenium ($Cp^*_2Co^+$) as an Ultra-Stable Cation for Polymer Hydroxide-Exchange Membranes

Received: 22 May 2015
Accepted: 01 June 2015
Published: 29 June 2015

Shuang Gu[1], Junhua Wang[1], Robert B. Kaspar[1], Qianrong Fang[1], Bingzi Zhang[1], E. Bryan Coughlin[2] & Yushan Yan[1]

Hydroxide (OH^-)-exchange membranes (HEMs) are important polymer electrolytes enabling the use of affordable and earth-abundant electrocatalysts for electrochemical energy-conversion devices such as HEM fuel cells, HEM electrolyzers, and HEM solar hydrogen generators. Many HEM cations exist, featuring desirable properties, but new cations are still needed to increase chemical stability at elevated temperatures. Here we introduce the permethyl cobaltocenium [$(C_5Me_5)_2Co(III)^+$ or $Cp^*_2Co^+$] as an ultra-stable organic cation for polymer HEMs. Compared with the parent cobaltocenium [$(C_5H_5)_2Co(III)^+$ or Cp_2Co^+], $Cp^*_2Co^+$ has substantially higher stability and basicity. With polysulfone as an example, we demonstrated the feasibility of covalently linking $Cp^*_2Co^+$ cation to polymer backbone and prepared $Cp^*_2Co^+$-functionalized membranes as well. The new cation may be useful in designing more durable HEM electrochemical devices.

Polymer hydroxide (OH^-)-exchange membranes (HEMs) are attractive electrolytes for electrochemical energy conversion devices such as fuel cells[1–18], electrolyzers[19,20], and solar hydrogen generators[21], largely due to their intrinsic compatibility with non-precious-metal catalysts[2,22] and superior CO_2 tolerance[23] compared to liquid alkaline electrolytes[24]. The active hydroxide-conducting component of an HEM is a cation that is covalently linked to a polymer backbone. Organic cations based on nitrogen [ammonium[25,26], pyridinium[27], guanidinium[28,29], imidazolium[6,30]], phosphorus [phosphonium[3,8]], sulfur [sulfonium[31]], and ruthenium [bis(terpyridine)ruthenium[7]] have been introduced, featuring specific HEM properties including improved solubility[3], enhanced thermal stability[31], and increased basicity[32]. New cations with chemical stability at elevated temperatures (>80 °C[33,34]) are still desired to reduce CO_2 poisoning, increase catalyst activity, and improve heat management in HEM electrochemical devices.

Alkali metal cations (*e.g.*, Li^+, Na^+, and K^+) provide the highest OH^- conductivity and show excellent stability, but at present cannot be covalently tethered to a polymer backbone for HEM applications[35]. Organic bis(cyclopentadienyl) metallocenium cations based on VIIIB family metals [$(C_5H_5)_2M(III)^+$ or $Cp_2M(III)^+$, M = Co, Rh, Ir, or Mt] satisfy the 18-valence electron stability rule and resemble alkali metal cations: They bear one unit of positive charge, may be precipitated by the addition of excess anions, and with hydroxide as counter-ion absorb CO_2 and water from ambient air[36]. In particular, cobalt is the smallest atom in the VIIIB family and forms the strongest metal-ring bonds, resulting in the most stable metallocenium cation, Cp_2Co^+ (cobaltocenium)[37]. While Cp_2Co^+ has been used in strongly basic anion-exchange resins[38,39] and water-soluble redox-active oligomers/polymers[40,41], none of these compounds appears suitable for HEM applications. In addition, the stability of Cp_2Co^+ may be still limited due to its unsubstituted Cp rings.

[1]Department of Chemical & Biomolecular Engineering, Center for Catalytic Science and Technology, University of Delaware, Newark, Delaware 19716, USA. [2]Department of Polymer Science and Engineering, University of Massachusetts, Amherst, Massachusetts 01003, USA. Correspondence and requests for materials should be addressed to Y.S.Y. (email: yanys@udel.edu)

Here we introduce the concept of using permethyl cobaltocenium $[(C_5Me_5)_2Co(III)^+$ or $Cp^*_2Co^+$, Fig. 1a,b] as a highly stable cation for polymer HEMs that are required in designing able and durable electrochemical devices.

Results

Cation stability: $Cp^*_2Co^+$ vs. Cp_2Co^+. Complete methylation of the Cp ring in $Cp^*_2Co^+$ enhances electron donation to the metal center, strengthening the metal-ring bond and delocalizing positive charge away from the metal center[42]. Calculations confirm that $Cp^*_2Co^+$ has a lower heat of formation (ΔH_f) than Cp_2Co^+, suggesting stronger bonding: 499 *vs.* 775 kJ mol^{-1} (a 36% reduction), as predicted by the semi-empirical quantum chemistry software MOPAC2012 (Table 1). The same calculation confirms that the charge on cobalt (δ_{Co}) is lower in $Cp^*_2Co^+$ than in Cp_2Co^+: +0.988 *vs.* +1.058 *e* (a 6.6% reduction). (Note that the overall system charge remains exactly +1 for both cations, regardless of delocalization.) This reduced charge is consistent with the substantial negative shift (*ca.* 600 mV) in redox potential (φ) observed for $Cp^*_2Co(III)^+/Cp^*_2Co(II)$ *vs.* $Cp_2Co(III)^+/Cp_2Co(II)$ (−1.24 V *vs.* −0.63 V, referring to the standard hydrogen electrode, SHE, with CH_2Cl_2 as solvent[43]).

The reduced positive charge on the metal center makes $Cp^*_2Co^+$ less susceptible to nucleophilic attack by hydroxide, which is, in general, the first step in HEM degradation. In addition to the electronic effect, steric hindrance[42] from the methyl groups in the Cp^* ligands may also further protect $Cp^*_2Co^+$ from hydroxide attack. The difference in steric hindrance between $Cp^*_2Co^+$ and Cp_2Co^+ can be quantified[6] by comparing the accessible angle (θ) that is formed by the cobalt center and the edges of circumcircle of hydrogen atoms (Fig. S1). Cp_2Co^+ has an accessible angle of 72.4° while $Cp^*_2Co^+$ has much smaller accessible angles of 40.3–49.6° (Table 1). The smaller accessible angle reduces the chance for the cobalt atom to be attacked.

Indeed, a high-temperature alkaline stability test (at 140 °C in 1 M NaOD/D_2O) showed that $Cp^*_2Co^+$ is significantly more stable than Cp_2Co^+. After six weeks (1,000 hours) only 8.5% of the initial $Cp^*_2Co^+$ had been found to degrade (^{13}C NMR, Fig. S2) whereas Cp_2Co^+ degraded completely after only one week (Fig. S3). Further, $Cp^*_2Co^+$ showed no change in UV-vis absorption after the stability test (Fig. S4). For comparison, a typical ammonium cation (trimethyl benzylammonium) degraded by 18% in 24 hours (Fig. S5). $Cp^*_2Co^+$ demonstrates a level of stability that has not been achieved by any known HEM cations (Fig. 2).

The reduced charge on cobalt also improves the basicity of the cation hydroxide, since weakened cation-anion interaction favors dissociation. Indeed, the base dissociation constant (K_b) is much larger for $Cp^*_2Co^+OH^-$ than for $Cp_2Co^+OH^-$: $pK_b = 2.7$ *vs.* 5.4 (a 500-fold increase in K_b, Table 1), as measured by correlating OH^- concentration with total organic base concentration in aqueous solution (Table S1 and Fig. S6). Improved basicity is expected to increase the hydroxide conductivity of the corresponding HEMs.

Superior stability and basicity suggest that $Cp^*_2Co^+$ is a much more desirable cation than Cp_2Co^+ for HEM applications.

Synthetic strategy for $Cp^*_2Co^+$-PSf polymer. $Cp^*_2Co^+$-PSf was synthesized by a diamine-bridge strategy (Fig. S7). The feasibility of this approach was established by a series of small-molecule model reactions (bromination, Fig. S8; anion exchange, Fig. S9; amination, Fig. S10; and cation incorporation, Fig. S11), in which benzyl chloride functioned as a surrogate for the halomethylated polymer. The $Cp^*_2Co^+$ cation was first brominated to introduce a single halomethyl group. In addition to ^1H NMR spectroscopy (Fig. S8), the bromination step was further confirmed by ^{13}C NMR (Fig. S12) and mass spectroscopy (Fig. S13, no sign of multiple bromination). In parallel, one amine group from hexamethylenediamine (HMDA) was linked to benzyl chloride by amination (leaving the other amine group intact). Then, the remaining unreacted amine group from HMDA was used to link the brominated $Cp^*_2Co^+$. Reaction conditions for all steps were optimized (yield >95%, ^1H NMR spectroscopy).

In a similar manner, $Cp^*_2Co^+$-PSf was synthesized (Figs. S14 and S15) and then membranes were prepared. Unlike the small-molecule model reaction, proper reaction conditions are critical for amination of polysulfone. Firstly, a low reaction temperature (*e.g.*, 20 °C) avoids the ammonolysis that leads to polysulfone depolymerization (observed at 40 °C and higher). Secondly, a large excess of amine (*e.g.*, 20 equiv.) avoids cross-linking in which one amine molecule reacts with two chloromethyl groups. Once cross-linked, the polymer becomes insoluble, and is no longer suitable for further reactions.

Note that the hydrophobic[44,45] PF_6^- anion in Br-$Cp^*_2Co^+PF_6^-$ must be exchanged for a hydrophilic anion (*e.g.*, Cl^-) prior to linking the cation to the backbone, due to the difficulty of exchanging PF_6^- for the ultimately desired OH^- in polyelectrolytes[7]. The counter-ion was later exchanged from Cl^- to OH^- with 1 M KOH. The $Cp^*_2Co^+$-PSf membranes were found be to flexible, uniform in thickness, and transparent (Fig. 3a).

Microstructure and properties of $Cp^*_2Co^+$-PSf membranes. Due to the presence of cobalt, high-contrast transmission electron microscopy (TEM) images were obtained without the need to employ a dye anion (*e.g.*, $PdCl_4^{2-}$ [46] or WO_4^{2-} [16]), directly revealing detailed features of the membrane microstructure (Fig. S16a). Overall, the hydrophilic (dark) and hydrophobic (light) domains are homogenously interspersed, which is essential to simultaneously provide ionic conduction and mechanical robustness[16].

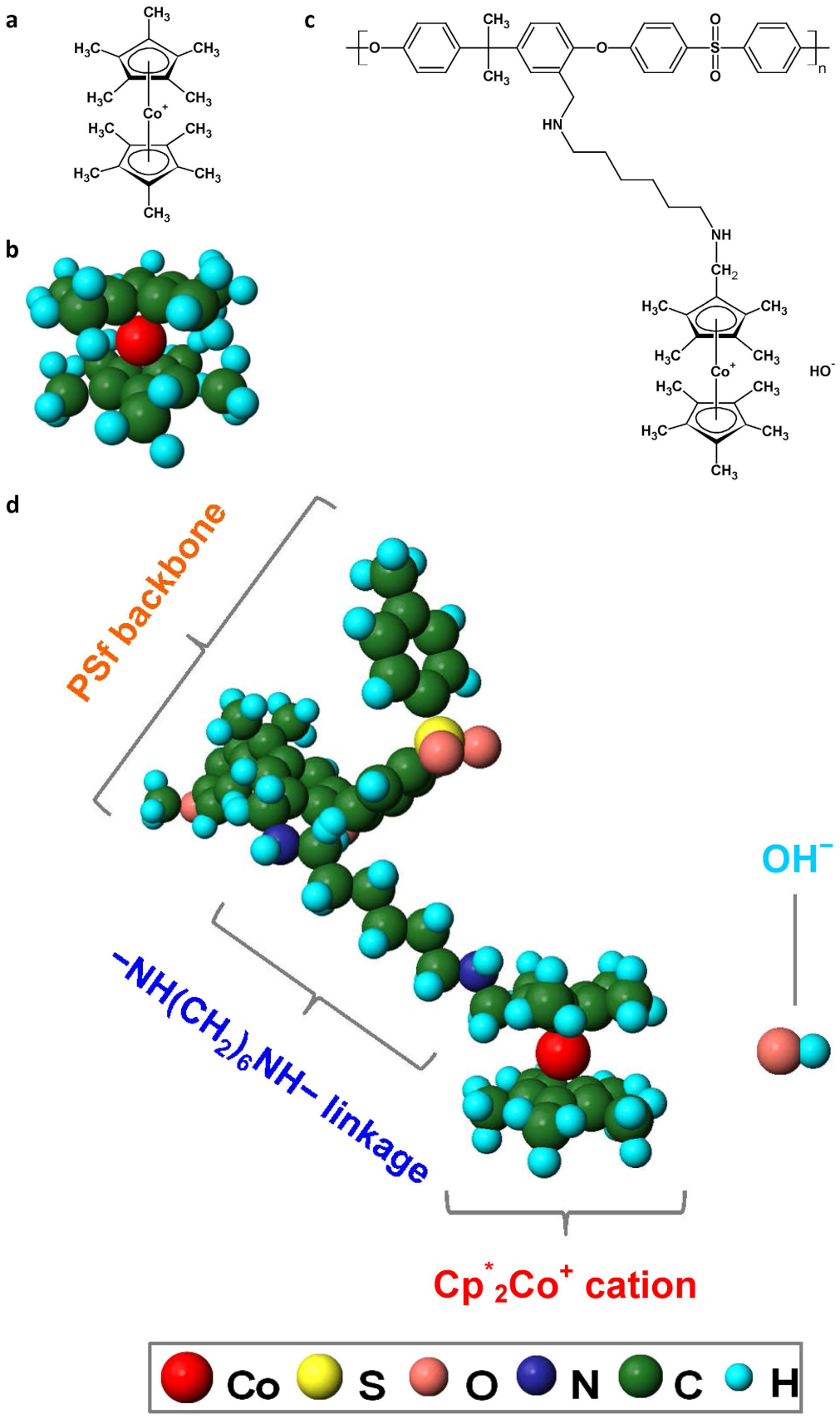

Figure 1. Structure of $Cp^*_2Co^+$ cation and $Cp^*_2Co^+$-functionalized polysulfone ($Cp^*_2Co^+$-PSf). (**a**) Chemical structure of $Cp^*_2Co^+$. (**b**) Molecular structure of $Cp^*_2Co^+$. (**c**) Chemical structure of $Cp^*_2Co^+$-PSf. (**d**) Molecular structure of $Cp^*_2Co^+$-PSf (one repeat unit of polysulfone shown, predicted by the software MOPAC and drawn in Jmol, version 13.0).

Cation	ΔH_f[a] (kJ mol^{-1}, cation)	δ_{Co}[b] (*e*, or 1.602 × 10^{-19} C)	φ[c] (V *vs.* SHE)	θ[d] (degree)	pK_b[e] (for cation hydroxide)
$Cp^*_2Co^+$	499	+0.988	−1.24[43]	40.3–49.6	2.7
Cp_2Co^+	775[f]	+1.058	−0.63[43]	72.4	5.4

Table 1. Comparison between $Cp^*_2Co^+$ and Cp_2Co^+. [a]ΔH_f: heat of formation, predicted by the software MOPAC2012 (Stewart Computational Chemistry). [b]δ_{Co}: partial charge at the cobalt atom, predicated by the same software. [c]φ: formal reductive potential of cation in CH_2Cl_2. [d]θ: accessible angle formed by cobalt and the edges of the circumcircles of hydrogen atoms in cation (Fig. S1). [e]K_b: base dissociation constant for cation hydroxide (Fig. S6). [f]This calculated value is close to the measured value reported in literature (823 kJ mol^{-1} [68]).

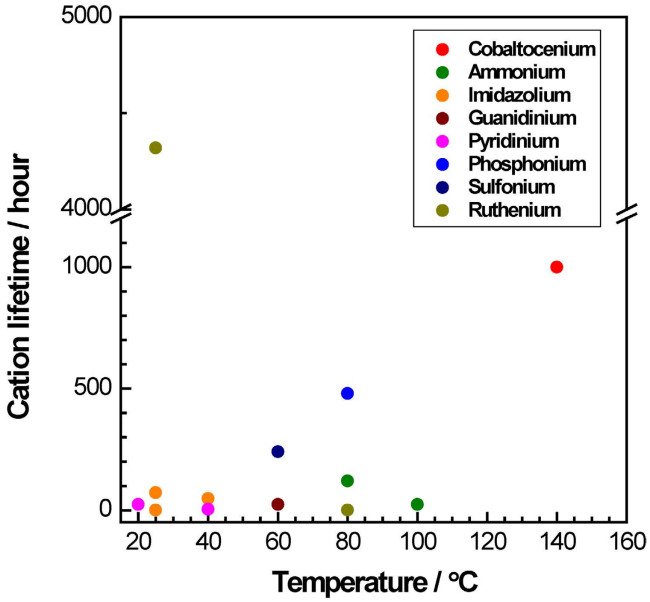

Figure 2. Alkaline stability of $Cp^*_2Co^+$ and other reported cations. Test conditions: 1 M KOD or NaOD in D_2O, 20% degradation threshold on ^{1}H NMR basis (unless otherwise noted). Cobaltocenium: $Cp^*_2Co^+$ (^{13}C NMR spectroscopy, this work). Ammonium: benzyl-trimethylammonium (*btm*Am) [80 °C in 1 M NaOD/(D_2O+CD_3OD)[8] and 100 °C in 1 M NaOD/D_2O, this work]. Imidazolium: benzyl-1-methyl-limidazolium (*bm*Im)[67], 1,3-dimethyl-2-phenyl-benzimidazolium (*dmp*BIm) (0.3 M KOH)[6], 1,3-dimethyl-2-(2,4,6-trimethylphenyl)-benzimidazolium (*dmtmp*BIm) (1.3 M KOH)[6]. Guanidinium: benzyl-pentamethylguanidium (*bpm*Gu) (this work). Pyridinium: benzylpyridinium (*b*Py) (this work). Phosphonium: tetrakis(dialkylamino)phosphonium (*tkdaa*Ph) [1 M NaOD/(D_2O+CD_3OD)][8]. Sulfonium: (4-methoxyphenyl)-diphenylsulfonium (*mopdp*Su)[31]. Ruthenium: bis(terpyridinine)ruthenium (*ttp*Ru) (UV-vis spectroscopy). The chemical structures of those cations are shown in Table S3. ^{1}H NMR spectra of *btm*Am, *bpm*Gu, and *b*Py are not shown.

The hydrophilic domains show an average size of 15 nm, similar to those in typical ammonium-based membranes (10–30 nm) with the same polysulfone backbone and similar ion exchange capacity (IEC, 1.14 mmol/g)[46]. The presence of cobalt was also confirmed by energy dispersive X-ray (EDX) spectroscopy during imaging (Fig. S16b). High tensile strength (40 MPa with 10% elongation at break, Fig. 3b) shows that the membrane is strong and robust. Under similar test conditions, the commercial proton exchange membrane (PEM) Nafion® 212 is half as strong (around 20 MPa[47]).

Two membranes of different degrees of functionalization (DFs, 100% and 123%) were characterized (Table 2). Both hydroxide conductivity and water uptake increase with ion exchange capacity (IEC), as with HEMs based on other cations. Note that the measured IECs are very close to the theoretical ones: 1.04 *vs.* 1.09 mmol g^{-1} for $Cp^*_2Co^+$-PSf100 membrane; 1.16 *vs.* 1.20 mmol g^{-1} for $Cp^*_2Co^+$-PSf123 membrane. Such an agreement indicates the $Cp^*_2Co^+$ cations in $Cp^*_2Co^+$-PSf membranes are fully functional. For comparison, HEMs with similar theoretical IEC and similar backbone (when available) but different cations are summarized in Table 2. The $Cp^*_2Co^+$-PSf membranes are similar to other membranes in terms of hydroxide conductivity (10–22 *vs.* 0.19–45 mS cm^{-1}) and water uptake (41%–68% *vs.* 8.2%–240%) in deionized water at room temperature, as well as IEC-normalized hydroxide conductivity

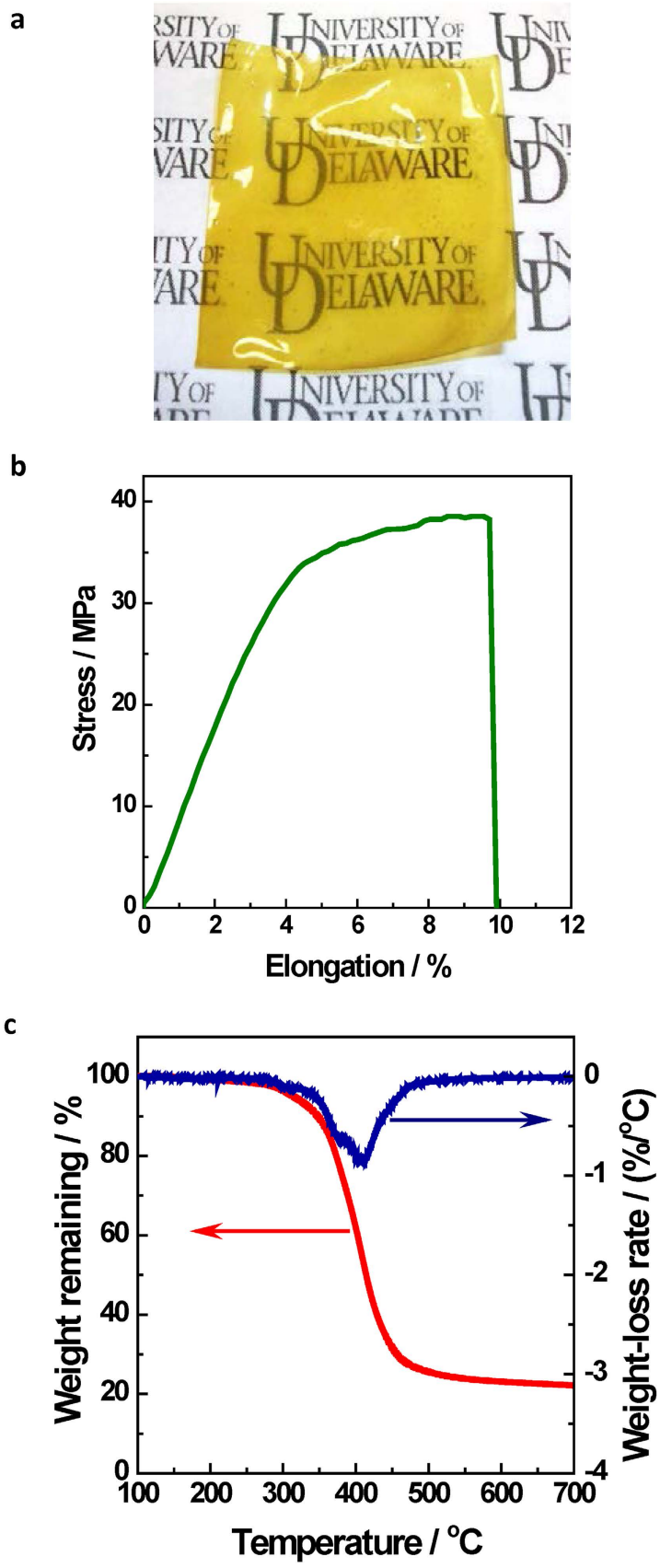

Figure 3. Characterization of $Cp^*_2Co^+$-PSf membrane. (**a**) Photograph (2" x 2", 100 μm thick). (**b**) Dynamic mechanical analysis (DMA) test curve (ambient humidity and temperature, 10 mm min^{-1} cross-head speed). (**c**) Thermal gravimetric analysis (TGA) and derivative thermal gravimetric (DTG) curves (10 °C min^{-1}, nitrogen atmosphere).

Cation	HEM[a]	IEC[b] (mmol/g)	HC[c] (mS/cm)	HC_{IEC}[d] (mS·g/cm·mmol)	WU[e] (%)	T_{OD}[f] (°C)	Ref.
Cobaltocenium	$Cp^*_2Co^+$-PSf123	1.20	22	18	68	305	This work
	$Cp^*_2Co^+$-PSff100	1.09	10	9.2	41		This work
Ammonium	*btm*Am-PSf58, 64[g]	1.08, 1.18	11, 19	10, 19	150, 240	150 (air)	2,46
	*bte*Am-PEK[h]	N/A	14	—	17	200	69
	*ptm*Am-PSf70, 100[i]	1.01, 1.32	15, 26	15, 20	8.7, 12	N/A	70
	*badm*Am-PPO20, 30[j]	1.08, 1.48	7, 14	6.5, 9.5	8.2, 14	N/A	71
	*dbdm*Am-PSf[k]	1.21	11	8.8	N/A	175	72
	*bdabco*Am-PSf[l]	N/A	22	—	N/A	N/A	73
	*bdmp*Am-PSf67[m]	1.23	11 (50 °C)	7.3	50	N/A	74
	*pdm*Am-PDDA39[n]	1.24	0.19	0.15	21	285 (Cl^-)	75
	*mam*Am-PBI50, 84[o]	1.15, 1.68	0.6, 2.9	0.52, 1.7	28, 50	160	76
	*btam*Am-PSt[p]	N/A	21	—	21	150	49
Imidazolium	*bm*Im-PSf66, 80[q]	1.28, 1.39	9, 16	7.0, 11	25, 8.5	140, 258	77,78
	*am*Im-PStAE20, 30[r]	0.80, 1.20	25, 31	31, 26	87, 116	210	79
	*bdm*Im-PETFE[s]	1.70	17 (HCO_3^-)	10	32 (Cl^-)	N/A	80
	*adm*Im-PFS200[t]	1.04	24	23	17	220	56
	*aam*Im-PStAE60, 80[u]	1.12, 1.50	5, 12	4.5, 8	41, 65	220	57
	*btmtmop*Im-PPO39[v]	1.36	34	25	125	N/A	81
	*dmp*BIm-PBI[w]	N/A	N/A	—	N/A	230	82
	*dmtmp*BIm-PBI64, 80[x]	1.00, 1.50	13.2, 10.1	13.2, 6.7	82, 119	N/A	6
Guanidinium	*bpm*Gu-bpPSf40, 60[y]	0.86, 1.21	5, 12	5.8, 9.9	12, 17	165	28
	*apm*Gu-PPS100[z]	1.39	22	16	32	200	55
	*ppm*Gu-fPSf85[aa]	1.03	21	20	10	N/A	29
Pyridinium	*a*Py-PVPSt50[ab]	1.76	0.6	0.76	30	230 (Br^-)	27
	*b*Py-PSt34[ac]	1.29	14	11	N/A	130 (DSC)	83
Phosphonium	*bttmop*Ph-PSf124, 152[ad]	1.09, 1.17	27, 45	25, 38	70, 137	187	3,32,48
	*tkdaa*Ph-PCoe17[ae]	0.93	22	24	52	N/A	8
Sulfonium	*mopdp*Su-PSf46[af]	0.69	15	22	27	242	31
Ruthenium	*ttp*Ru-PN9, 17[ag]	1.00, 1.40	14, 29	14, 21	30, 126	N/A	7

Table 2. Membrane properties of different cation-based HEMs (polysulfone backbone when available, chemical structures of cations shown in Table S3). [a]The number at the end of the name indicates degree of functionalization. [b]Ion exchange capacity based on theoretical calculation. [c]Hydroxide conductivity in deionized water at room temperature. [d]IEC-normalized hydroxide conductivity. [e]Water uptake. [f]Onset decomposition temperature from TGA test (N_2 atmosphere, 10 °C min^{-1}). [g]Benzyl-trimethylammonium (*btm*Am). [h]Benzyl-triethylammonium (*bte*Am), poly(ether ketone) (PEK). [i]Phenyl-trimethylammonium (*ptm*Am). [j]Benzyl-alkyl-dimethylammonium (*badm*Am), poly(phenylene oxide) (PPO). [k]Dibenzyl-dimethylammonium (*dbdm*Am). [l]Benzyl-1,4-diazabicyclo-[2.2.2]-octane-ammonium (*bdabco*Am). [m]Benzyl-(1,4-dimethyl)piperazine-ammonium (*bdmp*Am). [n]Pyrrolidine-dimethylammonium (*pdm*Am), poly(diallyldimethylammonium) (PDDA). [o]Morpholine-alkyl-methylammonium (*mam*Am), polybenzimidazole (PBI). [p]Benzyl-1,3,5-triazine-methylammonium (*btam*Am), polystyrene (PSt). [q]Benzyl-1-methyl-imidazolium (*bm*Im). [r]Alkyl-1-methyl-imidazolium (*am*Im), crosslinked poly(styrene acrylonitrile ethylene) (PStAE). [s]Benzyl-1,2-dimethyl-imidazolium (*bdm*Im), grafted poly(ethylene tetrafluoroethylene) (PETFE) backbone. [t]Alkyl-1,2-dimethyl-imidazolium (*adm*Im), poly(fluorene sulfone) (PFS). [u]Alkyl-1-alkyl-2-methyl-imidazolium (*aam*Im). [v]Benzyl-1,4,5-trimethyl-2-(2,4,6-trimethoxyphenyl)-limidazolium (*btmtmop*Im). [w]1,3-Dimethyl-2-phenyl-benzimidazolium (*dmp*BIm). [x]1,3-Dimethyl-2-(2,4,6-Trimethylphenyl)-benzimidazolium (*dmtmp*BIm). [y]Benzyl-pentamethylguanidinium (*bpm*Gu), biphenylene-type polysulfone (bpPSf). [z]Alkyl-pentamethylguanidinium (*apm*Gu), poly(phenolphthalein sulfone) (PPS). [aa]Phenyl-pentamethylguanidinium (*ppm*Gu), fluorinated polysulfone (fPSf). [ab]Alkylpyridinium (*a*Py), poly(vinylpyridine-styrene) (PVPSt). [ac]Benzylpyridinium (*b*Py), crosslinked backbone. [ad]Benzyl-tris(2,4,6-trimethoxyphenyl)-phosphonium (*bttmop*Ph). [ae]Tetrakis(dialkylamino)phosphonium (*tkdaa*Ph), polycyclooctene (PCoe). [af](4-Methoxyphenyl)-diphenylsulfonium (*mopdp*Su). [ag]Bis(terpyridinine)ruthenium (*btp*Ru), polynorbornene (PN).

(HC_{IEC}, 9.2–18 *vs.* 0.15–38 mS·g cm^{-1} $mmol^{-1}$), suggesting similar cation basicity and hydroxide conduction efficiency. As expected, hydroxide conductivity of $Cp^*_2Co^+$-PSf membranes increases with temperature. E.g., the hydroxide conductivity of $Cp^*_2Co^+$-PSf123 membranes reached 49 and 64 mS cm^{-1} at 60 and 80 °C, respectively.

Thermal and alkaline stability of $Cp^*_2Co^+$-PSf membranes. The membranes showed very high thermal stability, consistent with the aforementioned stability of the $Cp^*_2Co^+$ cation. The onset of decomposition temperature of 305 °C (Fig. 3c) is the highest among all reported HEMs: *e.g.*, 60 °C higher than a sulfonium-functionalized PSf[31], 120 °C higher than a phosphonium-functionalized PSf[48], or 150 °C higher than ammonium-functionalized PSfs[46,49]. Note that the thermal gravimetric analysis (TGA) data only reflect short-term thermal stability and are only useful for comparison under similar test conditions.

The $Cp^*_2Co^+$-PSf membranes also showed improved alkaline stability: At 80 °C in 1 M KOH, the IEC loss of $Cp^*_2Co^+$-PSf membranes was 18% and 27% of the initial value after 1,000 and 2,000 hours, respectively (Fig. S17). After the 1,000-hour stability test, solid-state ^{13}C NMR spectroscopy confirmed that $Cp^*_2Co^+$ functional groups remained almost unchanged (Fig. S18), but there were clear signs of PSf backbone scission. This result is consistent with that of a recent study[50], and it further highlights the need for more stable backbones in developing next-generation highly durable HEMs.

Under a more aggressive test at 100 °C for 2,000 hours, the IEC lost was about 50% for $Cp^*_2Co^+$-PSf membranes. Considering that higher test temperature leads to shorter membrane lifetime, the membrane lifetime is plotted against the test temperature (Fig. S19). With 20% loss of initial IEC as the failure criterion, $Cp^*_2Co^+$-PSf membranes are more stable than all other cation-based HEMs reported to date.

Discussion

Polysulfone was used as the polymer backbone in this work primarily to demonstrate linking $Cp^*_2Co^+$ to polymer and to compare $Cp^*_2Co^+$ to other cations reported. However, polysulfone backbone is sensitive for HEM degradation[50,51], and more stable polymer backbones are needed to better match the stable $Cp^*_2Co^+$ cation. Very recently, alternative polymer backbones, such as polystyrene[52] and poly(phenylene)[53], have been shown to have better stability than polysulfone in alkaline media. In principle, the synthesis reported here may be modified to employ those more stable polymer backbones. The incorporation of $Cp^*_2Co^+$ cation to more stable polymer backbones and the synthesis and stability of their resulting membranes warrant important future research.

In the amination step, the chain length of the diamine linker between the polymer backbone and the $Cp^*_2Co^+$ cation was found to affect membrane flexibility, likely resulting from the incompatibility between the rigid hydrophobic polymer backbone and the bulky hydrophilic cation. Increasing the chain length (*e.g.*, ethylene[54], propylene[54,55], and hexamethylene[56–58]) between cation and backbone helps alleviate this incompatibility. Indeed, HMDA, with six carbon atoms and two nitrogen atoms, was found to be a good choice for preparing flexible, robust membranes.

In the cation incorporation step, although Br-$Cp^*_2Co^+PF_6^-$ could react at two possible amine sites — either close to the polymer backbone (the basal secondary amine) and or at the end of side chain (the terminal primary amine) (Fig. S7) — a reaction was only observed at the terminal site, even for the less-hindered model molecule (Fig. S10). Such good selectivity results from strong steric hindrance in the bulky Br-$Cp^*_2Co^+PF_6^-$ molecule and higher nucleophilicity of the terminal amine group (pK_a of amines' conjugate acids: 10.21 and 10.21 for the basal amine *vs.* 9.26 and 9.93 for the terminal amine, of HMDA-aminated chloromethylated polysulfone polymer and HMDA-aminated benzyl chloride small molecule, respectively; calculated by the MarvinSketch software, Table S2).

During the model cation durability test, ^{13}C instead of ^1H NMR spectroscopy was used to monitor stability because both $Cp^*_2Co^+$ and Cp_2Co^+ undergo rapid H-D isotopic exchange upon exposure to alkaline media, rendering ^1H spectroscopy inappropriate for accessing stability[52]. Figs. S20 and S21 show the degree of H-D isotopic exchange is 78% and 29% for $Cp^*_2Co^+$ and Cp_2Co^+, respectively, under the same test conditions (60 °C, 40% KOH/D_2O in methanol, 30 min). This difference in degree of exchange is consistent with the observation from the literature that methyl protons are slightly more acidic than ring protons in cobaltocenium [p*K*a in methanol: 22.7 for methyl protons of 1,1'-dimethyl-cobaltocenium, $(1\text{-Me-Cp})_2Co^+$, *vs.* 23.9 for ring protons of Cp_2Co^+][59,60].

Table 2 summarizes the HEM samples with similar backbone and IECs for the purpose of comparing different cations. It is noted that HEMs with very high hydroxide conductivity have been reported. In general, high conductivity can be achieved by providing either high IEC or high efficiency of hydroxide conduction. With high IECs (> 2.0 mmol g^{-1}), HEMs exhibited high hydroxide conductivities (at ~20 °C unless otherwise noted) such as 43, 50, 65, 67, and 68.7 mS cm^{-1} for a *badm*Am-based PPO (2.75 mmol g^{-1})[9], a *btm*Am-based fluorenyl-containing poly(ether sulfone ketone) (2.54 mmol g^{-1}, 30 °C)[61], a *btm*Am-based di-fluorinated bpPSf (2.62 mmol g^{-1})[62], a *bpm*Gu-based bpPSf (2.15 mmol g^{-1})[28], and a *badm*Am-based cross-linked polyalkylene (2.3 mmol g^{-1})[5], respectively. High conductivities can also be realized with relatively low IECs via methods that likely improve the efficiency of hydroxide conduction. Examples include the use of architecture of aliphatic side chain (45 mS cm^{-1}, 30 °C, with 1.0 mmol g^{-1} for a *btm*Am-based hexyl-modified PSf)[13], saturated aliphatic backbone (48 mS cm^{-1} with 1.5 mmol g^{-1} for a trimethyl ammonium-based polyalkylene)[63], all-benzene-ring backbone (50 mS cm^{-1} with 1.57 mmol g^{-1} for a *btm*Am-based poly(phenylene)[64], hydrogen-bonding group (1,2,3-triazole) (62 mS cm^{-1} with

1.8 mmol g^{-1} for a trimethyl ammonium-based triazole-containing PPO)[65], and block copolymer backbone (80 mS cm^{-1} with 1.93 mmol g^{-1} for a poly(fluorenyl sulfone)-co-PSf)[16].

In summary, $Cp^*_2Co^+$ shows improved stability and basicity compared with Cp_2Co^+, making $Cp^*_2Co^+$ an ultra-stable cation for polymer HEMs. We have also incorporated $Cp^*_2Co^+$ cations to a typical polymer backbone (polysulfone) and the resulting membranes exhibited enhanced (short-term) thermal stability and improved (long-term) alkaline stability. More stable polymer backbones are needed to better match the outstanding stability of $Cp^*_2Co^+$ cation; and the availability of such a stable organic cation might help to develop the next-generation affordable and durable HEM electrochemical devices.

Methods

Computational methods for calculating ΔH_f, δ_{Co}, and pK_a. Heat of formation in gas phase (ΔH_f) of the cation and partial charge at the cobalt atom (δ_{Co}) were calculated by the software MOPAC2012 (Stewart Computational Chemistry) through the graphical user interface Vega ZZ (version 3.0.1.22, Drug Design Laboratory at the University of Milan). The keyword CHARGE = 1 was used to specify the total charge of the cation, and the keyword PRECISE was used to tighten convergence criteria. Conjugate acid dissociation constants (K_a) of two amine groups (basal and terminal) in hexamethylenediamine connected to polysulfone polymer and a benzyl group were predicted using the pK_a module of the software MarvinSketch (version 5.12.3, ChemAxon Ltd.) through an empirically parameterized method based on partial charge distribution[66]. One repeat unit of polysulfone with hydrogen atoms as end-groups was used in place of the whole polymer for the pK_a calculation.

Experimental method for measuring pK_b. Consider the dissociation equilibrium of a general base: $MOH \Leftrightarrow M^+ + OH^-$. In the equilibrium state, $K_b = ([M^+]\cdot[OH^-])/[MOH]$, where K_b is the dissociation constant of the base; $[M^+]$, $[OH^-]$, and [MOH] are concentrations of dissociated M^+, dissociated OH^-, and undissociated MOH, respectively. When $[H^+]$ is neglected (reasonable in base), $[M^+] = [OH^-]$, so $K_b = [OH^-]/(C_0/[OH^-]-1)$, where C_0 is the initial concentration of MOH. K_b can be obtained from fitting the slope of the line of $[OH^-]$ vs. $(C_0/[OH^-]-1)$. The pH of $Cp^*_2Co^+OH^-$ and $Cp_2Co^+OH^-$ solutions was measured at different initial concentrations (ranging from 0.25 to 50 mM) and the slope was fitted to give K_b. Pure $Cp^*_2Co^+OH^-$ and $Cp_2Co^+OH^-$ were prepared by ion exchange of $Cp^*_2Co^+PF_6^-$ and $Cp_2Co^+PF_6^-$, respectively, with a strongly-basic fast-kinetics anion-exchange resin (Amberjet® 4200, Dow Chemical Co.), which had been pre-exchanged with hydroxide in 50 wt% water : 50 wt% methanol, followed by filtration to remove resin and evaporation to remove solvent.

Synthesis of Br-$Cp^*_2Co^+Cl^-$compound. Permethyl-cobaltocenium hexafluorophosphate ($Cp^*_2Co^+PF_6^-$) was brominated by N-bromosuccinimide (NBS) with dibenzoyl peroxide (BPO) as radical initiator and 1,1,2,2-tetrachloroethane (TCE) as solvent. Specifically, 0.474 g (1 mmol) of $Cp^*_2Co^+PF_6^-$ was dissolved in 10 ml TCE, and then 0.178 g (1 mmol) of NBS and 0.0121 g (0.05 mmol) of BPO were added into the solution. After 24 hours of reaction with stirring at 100 °C, brominated permethyl-cobaltocenium hexafluorophosphate (Br-$Cp^*_2Co^+PF_6^-$) was precipitated by pouring the reacted solution into excess diethyl ether. Subsequently, the Br-$Cp^*_2Co^+PF_6^-$ precipitate was filtered, washed thoroughly with diethyl ether, and dried in vacuum at room temperature. The degree of bromination was found to be 95% by NMR spectroscopy (^{1}H, Fig. S8 and ^{13}C, Fig. S12) and mass spectroscopy (Fig. S13). Second, the Br-$Cp^*_2Co^+PF_6^-$ was ion exchanged with a strongly basic fast-kinetics anion exchange resin balanced with Cl^- to produce brominated permethyl-cobaltocenium chloride (Br-$Cp^*_2Co^+Cl^-$). Specifically, Br-$Cp^*_2Co^+PF_6^-$ was dissolved in deionized water and then the excess (20 equiv.) anion exchange resin (Amberjet® 4200 with chloride anion) was added into the solution. With stirring, the ion exchange was held at room temperature for 24 hours, and then the resin was removed by filtration. Br-$Cp^*_2Co^+Cl^-$ was obtained as a yellow powder by evaporating water from the filtrate. The anion exchange was confirmed by ^{19}F NMR spectroscopy with 97% replacement of PF_6^- by Cl^- (Fig. S9).

Synthesis of BAHA-$Cp^*_2Co^+Cl^-$ compound. First, benzyl chloride was aminated by excess (20 equiv.) hexamethylenediamine (HMDA). Specifically, 0.127 g (1 mmol) benzyl chloride was dissolved in 10 ml N-methyl-2-pyrrolidone (NMP), then 2.32 g (20 mmol) HMDA and 0.652 g (2 mmol) cesium carbonate were added into the solution. The amination reaction was carried out for 24 hours with stirring at room temperature, then the solvent was removed by adding excess diethyl ether, leaving behind the mixture of desired product (i.e., N-benzylhexane-1,6-diamine, BHDA) and residual HMDA. The HMDA was removed by addition of excess saturated K_2CO_3 aqueous solution. The leftover BHDA white power was thoroughly washed with deionized water, followed by drying at 40 °C for 48 hours under vacuum. The synthesis was confirmed by ^{1}H NMR spectroscopy with complete mono-amination (Fig. S10). Second, (6-(benzyl amino)hexylamino permethyl-cobaltocenium chloride (BAHA-$Cp^*_2Co^+Cl^-$) was synthesized by reacting BHDA with Br-$Cp^*_2Co^+Cl^-$. Specifically, 0.206 g (1 mmol) BHDA was dissolved in 10 ml NMP, and 0.444 g (1 mmol) Br-$Cp^*_2Co^+Cl^-$ was added into the solution. The reaction was carried out at 80 °C for 24 hours with stirring, then the solvent was removed by adding excess diethyl ether and the BAHA-$Cp^*_2Co^+Cl^-$ was obtained after washing by saturated K_2CO_3 aqueous solution and deionized water sequentially. The reaction was confirmed by ^{1}H NMR spectroscopy with complete conversion (Fig. S11) and complete selectivity for the terminal amine over the basal amine.

Synthesis of $Cp^*_2Co^+$-PSf polymer. First, chloromethylated polysulfone (CM-PSf) was synthesized with trimethylchlorosilane and paraformaldehyde as co-chloromethylating agent and stannic chloride as catalyst as reported in detail in our previous work[32]. Second, CM-PSf was aminated with excess HMDA similar to the case of benzyl chloride. Specifically, 0.502 g (1 mmol polysulfone repeat unit or 1.23 mmol chloromethyl group for 123% of DC) CM-PSf was dissolved in 10 ml NMP, then 2.85 g (24.6 mmol) HMDA and 0.802 g (2.46 mmol) cesium carbonate were added into the solution. The amination reaction was held at room temperature for 24 hours with stirring, then the HMDA-aminated polysulfone (HMDA-PSf) white powder was precipitated by pouring the reacted mixture into excess deionized water. After filtration and thorough washing with deionized water, the HMDA-PSf was dried at 40 °C for 48 hours under vacuum. The synthesized HMDA-PSf is completely soluble in organic solvents such as chloroform and NMP, and neither crosslinking nor depolymerization was found for the HMDA-PSf. The synthesis was confirmed by ^{1}H NMR spectroscopy with 96% conversion of the chloromethyl groups (Fig. S14).

Second, $Cp^*_2Co^+$-PSf was synthesized by reacting HMDA-PSf with Br-$Cp^*_2Co^+Cl^-$. Specifically, 0.600 g (1 mmol polysulfone repeat unit or 1.23 mmol terminal amine group) HMDA-PSf was dissolved in 10 ml NMP, then 0.546 g (1.23 mmol) Br-$Cp^*_2Co^+Cl^-$ was added into the solution. The reaction was completed by heating the mixture at 80 °C for 24 hours with stirring. The reacted solution was cast onto a glass plate and the $Cp^*_2Co^+$-PSf membranes were obtained after drying at 60 °C for 72 hours. The balancing anion of $Cp^*_2Co^+$-PSf membranes was exchanged with hydroxide by treatment in 1 M KOH at room temperature for 48 hours. After thorough washing and immersion in deionized water for another 48 hours to completely remove residual KOH, the membranes were ready for use. The synthesis of $Cp^*_2Co^+$-PSf was confirmed by solid-state ^{13}C NMR spectroscopy (Fig. S15).

References

1. Varcoe, J. R. & Slade, R. C. T. Prospects for alkaline anion-exchange membranes in low temperature fuel cells. *Fuel Cells* **5,** 187–200 (2005).
2. Lu, S. F. *et al.* Alkaline polymer electrolyte fuel cells completely free from noble metal catalysts. *P Natl Acad Sci Usa* **105,** 20611–20614 (2008).
3. Gu, S. *et al.* A Soluble and Highly Conductive Ionomer for High-Performance Hydroxide Exchange Membrane Fuel Cells. *Angew Chem Int Edit* **48,** 6499–6502 (2009).
4. Clark, T. J. *et al.* A Ring-Opening Metathesis Polymerization Route to Alkaline Anion Exchange Membranes: Development of Hydroxide-Conducting Thin Films from an Ammonium-Functionalized Monomer. *J Am Chem Soc* **131,** 12888–12889 (2009).
5. Robertson, N. J. *et al.* Tunable High Performance Cross-Linked Alkaline Anion Exchange Membranes for Fuel Cell Applications. *J Am Chem Soc* **132,** 3400–3404 (2010).
6. Thomas, O. D. *et al.* A Stable Hydroxide-Conducting Polymer. *J Am Chem Soc* **134,** 10753–10756 (2012).
7. Zha, Y. P. *et al.* Metal-Cation-Based Anion Exchange Membranes. *J Am Chem Soc* **134,** 4493–4496 (2012).
8. Noonan, K. J. T. *et al.* Phosphonium-Functionalized Polyethylene: A New Class of Base-Stable Alkaline Anion Exchange Membranes. *J Am Chem Soc* **134,** 18161–18164 (2012).
9. Li, N. W., Leng, Y. J., Hickner, M. A. & Wang, C. Y. Highly Stable, Anion Conductive, Comb-shaped Copolymers for Alkaline Fuel Cells. *J Am Chem Soc* **135,** 10124–10133 (2013).
10. Zeng, R. *et al.* Alkaline ionomer with tuneable water uptakes for electrochemical energy technologies. *Energy Environ Sci* **4,** 4925–4928 (2011).
11. Deavin, O. I. *et al.* Anion-exchange membranes for alkaline polymer electrolyte fuel cells: comparison of pendent benzyltrimethylammonium- and benzylmethylimidazolium-head-groups. *Energy Environ Sci* **5,** 8584–8597 (2012).
12. Pan, J. *et al.* A strategy for disentangling the conductivity-stability dilemma in alkaline polymer electrolytes. *Energy Environ Sci* **6,** 2912–2915 (2013).
13. Pan, J. *et al.* Constructing ionic highway in alkaline polymer electrolytes. *Energy Environ Sci* **7,** 354–360 (2014).
14. Li, N. W. *et al.* Comb-shaped polymers to enhance hydroxide transport in anion exchange membranes. *Energy Environ Sci* **5,** 7888–7892 (2012).
15. John, J. *et al.* An Electrochemical Quartz Crystal Microbalance Study of a Prospective Alkaline Anion Exchange Membrane Material for Fuel Cells: Anion Exchange Dynamics and Membrane Swelling. *J Am Chem Soc* **136,** 5309–5322 (2014).
16. Tanaka, M. *et al.* Anion Conductive Block Poly(arylene ether)s: Synthesis, Properties, and Application in Alkaline Fuel Cells. *J Am Chem Soc* **133,** 10646–10654 (2011).
17. Varcoe, J. R. *et al.* Anion-exchange membranes in electrochemical energy systems. *Energ Environ Sci* **7,** 3135–3191 (2014).
18. Wang, Y. *et al.* Pt-Ru catalyzed hydrogen oxidation in alkaline media: oxophilic effect or electronic effect? *Energy Environ Sci* **8,** 177–181 (2015).
19. Xiao, L. *et al.* First implementation of alkaline polymer electrolyte water electrolysis working only with pure water. *Energy Environ Sci* **5,** 7869–7871 (2012).
20. Leng, Y. J. *et al.* Solid-State Water Electrolysis with an Alkaline Membrane. *J Am Chem Soc* **134,** 9054–9057 (2012).
21. Spurgeon, J. M. *et al.* Electrical conductivity, ionic conductivity, optical absorption, and gas separation properties of ionically conductive polymer membranes embedded with Si microwire arrays. *Energy Environ Sci* **4,** 1772–1780 (2011).
22. Gu, S. *et al.* An efficient Ag-ionomer interface for hydroxide exchange membrane fuel cells. *Chem Commun* **49,** 131–133 (2013).
23. Adams, L. A. *et al.* A carbon dioxide tolerant aqueous-electrolyte-free anion-exchange membrane alkaline fuel cell. *Chemsuschem* **1,** 79–81 (2008).
24. Gu, S., Xu, B. J. & Yan, Y. S. Electrochemical Energy Engineering: A New Frontier of Chemical Engineering Innovation. *Annu Rev Chem Biomol Eng* **5,** 429–454 (2014).
25. Agel, E., Bouet, J. & Fauvarque, J. F. Characterization and use of anionic membranes for alkaline fuel cells. *J Power Sources* **101,** 267–274 (2001).
26. Danks, T. N., Slade, R. C. T. & Varcoe, J. R. Comparison of PVDF- and FEP-based radiation-grafted alkaline anion-exchange membranes for use in low temperature portable DMFCs. *J Mater Chem* **12,** 3371–3373 (2002).
27. Huang, A. B., Xiao, C. B. & Zhuang, L. Synthesis and characterization of quaternized poly(4-vinylpyridine-co-styrene) membranes. *J Appl Polym Sci* **96,** 2146–2153 (2005).

28. Wang, J. H., Li, S. H. & Zhang, S. B. Novel Hydroxide-Conducting Polyelectrolyte Composed of an Poly(arylene ether sulfone) Containing Pendant Quaternary Guanidinium Groups for Alkaline Fuel Cell Applications. *Macromolecules* **43,** 3890–3896 (2010).
29. Kim, D. S., Labouriau, A., Guiver, M. D. & Kim, Y. S. Guanidinium-Functionalized Anion Exchange Polymer Electrolytes via Activated Fluorophenyl-Amine Reaction. *Chem Mater* **23,** 3795–3797 (2011).
30. Guo, M. L. *et al.* Synthesis and characterization of novel anion exchange membranes based on imidazolium-type ionic liquid for alkaline fuel cells. *J Membrane Sci* **362,** 97–104 (2010).
31. Zhang, B. Z. *et al.* Tertiary sulfonium as a cationic functional group for hydroxide exchange membranes. *RSC Adv* **2,** 12683–12685 (2012).
32. Gu, S. *et al.* Quaternary Phosphonium-Based Polymers as Hydroxide Exchange Membranes. *Chemsuschem* **3,** 555–558 (2010).
33. Pivovar, B. 2011 Alkaline Membrane Fuel Cell Workshop Final Report. National Renewable Energy Laboratory, Arlington, Virginia, (2011) Date of Access: 01/01/2013.
34. Sturgeon, M. R. *et al.* Hydroxide based Benzyltrimethylammonium Degradation: Quantification of Rates and Degradation Technique Development. *J Electrochem Soc* **162,** F366–F372 (2015).
35. Luo, H. Z. *et al.* Anion exchange membrane based on alkali doped poly(2,5-benzimidazole) for fuel cell. *Solid State Ionics* **208,** 52–55 (2012).
36. Wilkinson, G. & Cotton, F. A. Cyclopentadienyl and Arene Metal Compounds. *Prog Inorg Chem* **1,** 1–124 (1959).
37. Sheats, J. E., Hlatky, G. & Dickson, R. S. Stabilization of Negative Charge by the Cobalticinium Nucleus .3. Effect of Substituents on the Acidities of Hydroxy-Cobalticinium and Hydroxy-Rhodicinium Salts. *J Organomet Chem* **173,** 107–115 (1979).
38. Ito, T. & Kenjo, T. Ion-Exchange Properties of Anion-Exchanger Containing Cobalticinium Cations. *B Chem Soc Jpn* **41,** 1600-& (1968).
39. Ito, T. & Kenjo, T. A New Anion Exchanger Containing Cobalticinium Cation. *B Chem Soc Jpn* **41,** 614-& (1968).
40. Mayer, U. F. J., Gilroy, J. B., O'Hare, D. & Manners, I. Ring-Opening Polymerization of 19-Electron [2]Cobaltocenophanes: A Route to High-Molecular-Weight, Water-Soluble Polycobaltocenium Polyelectrolytes. *J Am Chem Soc* **131,** 10382-+ (2009).
41. Ren, L. X., Hardy, C. G. & Tang, C. B. Synthesis and Solution Self-Assembly of Side-Chain Cobaltocenium-Containing Block Copolymers. *J Am Chem Soc* **132,** 8874-+ (2010).
42. Robbins, J. L., Edelstein, N., Spencer, B. & Smart, J. C. Syntheses and Electronic-Structures of Decamethylmetallocenes. *J Am Chem Soc* **104,** 1882–1893 (1982).
43. Koelle, U. & Khouzami, F. Permethylated Electron-Excess Metallocenes. *Angew Chem Int Edit* **19,** 640–641 (1980).
44. O'Mahony, A. M. *et al.* Effect of Water on the Electrochemical Window and Potential Limits of Room-Temperature Ionic Liquids. *J Chem Eng Data* **53,** 2884–2891 (2008).
45. Terborg, L. *et al.* Ion chromatographic determination of hydrolysis products of hexafluorophosphate salts in aqueous solution. *Anal Chim Acta* **714,** 121–126 (2012).
46. Pan, J. *et al.* High-Performance Alkaline Polymer Electrolyte for Fuel Cell Applications. *Adv Funct Mater* **20,** 312–319 (2010).
47. Dai, H. *et al.* Properties and fuel cell performance of proton exchange membranes prepared from disulfonated poly(sulfide sulfone). *J Power Sources* **185,** 19–25 (2008).
48. Gu, S., Cai, R. & Yan, Y. S. Self-crosslinking for dimensionally stable and solvent-resistant quaternary phosphonium based hydroxide exchange membranes. *Chem Commun* **47,** 2856–2858 (2011).
49. Cao, Y. C., Wang, X., Mamlouk, M. & Scott, K. Preparation of alkaline anion exchange polymer membrane from methylated melamine grafted poly(vinylbenzyl chloride) and its fuel cell performance. *J Mater Chem* **21,** 12910–12916 (2011).
50. Arges, C. G. & Ramani, V. Two-dimensional NMR spectroscopy reveals cation-triggered backbone degradation in polysulfone-based anion exchange membranes. *P Natl Acad Sci Usa* **110,** 2490–2495 (2013).
51. Patel, N. B. & Patel, J. C. Synthesis and antimicrobial activity of Schiff bases and 2-azetidinones derived from quinazolin-4(3H)-one. *Arab J Chem* **4,** 403–411 (2011).
52. Nunez, S. A. & Hickner, M. A. Quantitative H-1 NMR Analysis of Chemical Stabilities in Anion-Exchange Membranes. *Acs Macro Letters* **2,** 49–52 (2013).
53. Choe, Y. K. *et al.* Alkaline Stability of Benzyl Trimethyl Ammonium Functionalized Polyaromatics: A Computational and Experimental Study. *Chem Mater* **26,** 5675–5682 (2014).
54. Zhang, Q. A. *et al.* Synthesis and alkaline stability of novel cardo poly(aryl ether sulfone)s with pendent quaternary ammonium aliphatic side chains for anion exchange membranes. *Polymer* **51,** 5407–5416 (2010).
55. Zhang, Q. A., Li, S. H. & Zhang, S. B. A novel guanidinium grafted poly(aryl ether sulfone) for high-performance hydroxide exchange membranes. *Chem Commun* **46,** 7495–7497 (2010).
56. Lin, B. C. *et al.* A Soluble and Conductive Polyfluorene Ionomer with Pendant Imidazolium Groups for Alkaline Fuel Cell Applications. *Macromolecules* **44,** 9642–9649 (2011).
57. Qiu, B. *et al.* Bis-imidazolium-based anion-exchange membranes for alkaline fuel cells. *J Power Sources* **217,** 329–335 (2012).
58. Hibbs, M. R. Alkaline Stability of Poly(phenylene)-Based Anion Exchange Membranes With Various Cations. *J Polym Sci Pol Phys* **51,** 1736–1742 (2013).
59. Bykova, E. V., Mukhina, T. A., Setkina, V. N. & Kursanov, D. N. Effect of Substituents on Rate of Protophilic Isotopic-Exchange of Hydrogen of Cobalticinium Salts. *Doklady Akademii Nauk Sssr* **214,** 329–331 (1974).
60. Sheats, J. E., Miller, W. & Kirsch, T. Stabilization of Negative Charge by Cobalticinium Nucleus. *J Organomet Chem* **91,** 97–104 (1975).
61. Tanaka, M., Koike, M., Miyatake, K. & Watanabe, M. Anion Conductive Aromatic Ionomers Containing Fluorenyl Groups. *Macromolecules* **43,** 2657–2659 (2010).
62. Wang, J. H. *et al.* Synthesis of Soluble Poly(arylene ether sulfone) Ionomers with Pendant Quaternary Ammonium Groups for Anion Exchange Membranes. *Macromolecules* **42,** 8711–8717 (2009).
63. Kostalik, H. A. *et al.* Solvent Processable Tetraalkylammonium-Functionalized Polyethylene for Use as an Alkaline Anion Exchange Membrane. *Macromolecules* **43,** 7147–7150 (2010).
64. Hibbs, M. R., Fujimoto, C. H. & Cornelius, C. J. Synthesis and Characterization of Poly(phenylene)-Based Anion Exchange Membranes for Alkaline Fuel Cells. *Macromolecules* **42,** 8316–8321 (2009).
65. Li, N. W., Guiver, M. D. & Binder, W. H. Towards High Conductivity in Anion-Exchange Membranes for Alkaline Fuel Cells. *Chemsuschem* **6,** 1376–1383 (2013).
66. Szegezdi, J. & Csizmadia, F. in *American Chemical Society Spring Meeting* (Chicago, IL, 2007).
67. Wang, J. H. *et al.* Stabilizing Imidazolium Cation for Hydroxide Exchange Membranes. *ChemSusChem* **6,** 2079–2082 (2013).
68. Opitz, J. Electron impact ionization of cobalt-tricarbonyl-nitrosyl, cyclopentadienyl-cobalt-dicarbonyl and biscyclopentadienyl-cobalt: appearance energies, bond energies and enthalpies of formation. *Int J Mass Spectrom* **225,** 115–126 (2003).
69. Zarrin, H., Wu, J., Fowler, M. & Chen, Z. W. High durable PEK-based anion exchange membrane for elevated temperature alkaline fuel cells. *J Membrane Sci* **394,** 193–201 (2012).
70. Li, N. *et al.* Phenyltrimethylammonium Functionalized Polysulfone Anion Exchange Membranes. *Macromolecules* **45,** 2411–2419 (2012).

71. Zhang, Y. M. *et al.* Novel fluoropolymer anion exchange membranes for alkaline direct methanol fuel cells. *J Colloid Interf Sci* **381,** 59–66 (2012).
72. Pan, J., Li, Y., Zhuang, L. & Lu, J. T. Self-crosslinked alkaline polymer electrolyte exceptionally stable at 90 degrees C. *Chem Commun* **46,** 8597–8599 (2010).
73. Wang, X. *et al.* A polytetrafluoroethylene-quaternary 1,4-diazabicyclo-[2.2.2]-octane polysulfone composite membrane for alkaline anion exchange membrane fuel cells. *Int J Hydrogen Energ* **36,** 10022–10026 (2011).
74. Arges, C. G. *et al.* Assessing the influence of different cation chemistries on ionic conductivity and alkaline stability of anion exchange membranes. *J Mater Chem* **22,** 3733–3744 (2012).
75. Valade, D., Boschet, F., Roualdes, S. & Ameduri, B. Preparation of Solid Alkaline Fuel Cell Binders Based on Fluorinated Poly(diallyldimethylammonium chloride)s [Poly(DADMAC)] or Poly(chlorotrifluoroethylene-co-DADMAC) Copolymers. *J Polym Sci Pol Chem* **47,** 2043–2058 (2009).
76. Xia, Z. J. *et al.* Polybenzimidazoles with pendant quaternary ammonium groups as potential anion exchange membranes for fuel cells. *J Membrane Sci* **390,** 152–159 (2012).
77. Ni, J. *et al.* Novel self-crosslinked poly(aryl ether sulfone) for high alkaline stable and fuel resistant alkaline anion exchange membranes. *Chem Commun* **47,** 8943–8945 (2011).
78. Yan, X. M. *et al.* Imidazolium-functionalized polysulfone hydroxide exchange membranes for potential applications in alkaline membrane direct alcohol fuel cells. *Int J Hydrogen Energ* **37,** 5216–5224 (2012).
79. Lin, B. C., Qiu, L. H., Lu, J. M. & Yan, F. Cross-Linked Alkaline Ionic Liquid-Based Polymer Electrolytes for Alkaline Fuel Cell Applications. *Chem Mater* **22,** 6718–6725 (2010).
80. Page, O. M. M. *et al.* The alkali stability of radiation-grafted anion-exchange membranes containing pendent 1-benzyl-2,3-dimethylimidazolium head-groups. *RSC Adv* **3,** 579–587 (2013).
81. Wang, J. H. *et al.* Stabilizing The Imidazolium Cation for Hydroxide Exchange Membranes. *Chemsuschem* **6,** 2079–2082 (2013).
82. Henkensmeier, D. *et al.* Polybenzimidazolium hydroxides - Structure, stability and degradation. *Polym Degrad Stabil* **97,** 264–272 (2012).
83. Zhang, C. X. *et al.* Microphase separated hydroxide exchange membrane synthesis by a novel plasma copolymerization approach. *J Power Sources* **198,** 112–116 (2012).

Acknowledgements

This work was supported by the MURI of the U.S. DOD under the contract W911NF-10-1-0520. S.G. thanks Mr. Jesse McAtee and Dr. Guangjin Hou in the Department of Chemistry and Biochemistry of University of Delaware for the help in mass spectroscopy study and in solid-state NMR spectroscopy investigation, respectively.

Author Contributions

S.G. designed the experiments. S.G. and J.H.W. performed the polymer synthesis experiments, K_b measurement, and membrane characterization. J.H.W. performed the model reaction experiments and TEM imaging. Q.R.F. and J.H.W. performed cation stability test. B.Z.Z. and J.H.W. performed NMR test. R.B.K. performed the computational predictions on partial charge, heat of formation, molecular structure, and p*K*a. E.B.C. designed the studies of benchmark ammonium degradation, mass spectroscopy, and H-D isotopic exchange experiments. S.G., E.B.C. and Y.S.Y. wrote the manuscript. Y.S.Y. directed the research work.

Additional Information

Supplementary information accompanies this paper at http://www.nature.com/srep

Competing financial interests: The authors declare no competing financial interests.

How to cite this article: Gu, S. *et al.* Permethyl Cobaltocenium ($Cp^*_2Co^+$) as an Ultra-Stable Cation for Polymer Hydroxide Exchange Membranes. *Sci. Rep.* **5**, 11668; doi: 10.1038/srep11668 (2015).